Force measurements show that uL4 and uL24 mechanically stabilize a fragment of 23S rRNA essential for ribosome assembly

LAURENT GEFFROY,[1,4] THIERRY BIZEBARD,[2] RYO AOYAMA,[3] TAKUYA UEDA,[3] and ULRICH BOCKELMANN[1]

[1]Nanobiophysics, ESPCI Paris, 75005 Paris, France

[2]Expression Génétique Microbienne, UMR8261 CNRS/Université Paris 7, IBPC, 75005 Paris, France

[3]Department of Computational Biology and Medical Sciences, Graduate School of Frontier Sciences, The University of Tokyo, FSB-401, Kashiwa, Chiba 277-8562, Japan

ABSTRACT

In vitro reconstitution studies have shown that ribosome assembly is highly cooperative and starts with the binding of a few ribosomal (r-) proteins to rRNA. It is unknown how these early binders act. Focusing on the initial stage of the assembly of the large subunit of the *Escherichia coli* ribosome, we prepared a 79-nucleotide-long region of 23S rRNA encompassing the binding sites of the early binders uL4 and uL24. Force signals were measured in a DNA/RNA dumbbell configuration with a double optical tweezers setup. The rRNA fragment was stretched until unfolded, in the absence or in the presence of the r-proteins (either uL4, uL24, or both). We show that the r-proteins uL4 and uL24 individually stabilize the rRNA fragment, both acting as molecular clamps. Interestingly, this mechanical stabilization is enhanced when both proteins are bound simultaneously. Independently, we observe a cooperative binding of uL4 and uL24 to the rRNA fragment. These two aspects of r-proteins binding both contribute to the efficient stabilization of the 3D structure of the rRNA fragment under investigation. We finally consider implications of our results for large ribosomal subunit assembly.

Keywords: ribosome assembly; single molecule; optical trap

INTRODUCTION

The ribosome is the essential molecular machine responsible for protein biosynthesis in all living organisms. While ribosome biogenesis in vivo can occur efficiently at temperatures of 37°C or less in a couple of minutes, in vitro reconstitution of the large subunit of the *Escherichia coli* ribosome (the 50S subunit) takes about 90 min and requires temperatures of ~50°C (Nierhaus 1991). A classical reason invoked to explain this difference is that in vivo ribosome assembly occurs cotranscriptionally, i.e., r-proteins bind to the rRNA during its synthesis.

In vivo the rRNA can thus sequentially interact with the r-proteins and fold; this is in strong contrast to in vitro, where the entire rRNA molecule is present from start. This could lead to an entropic advantage through an "assembly gradient" in vivo (the progress of rRNA transcription defines the progress of assembly) (Spillmann et al. 1977; Herold and Nierhaus 1987; Chen and Williamson 2013). In this respect, a crucial observation was that the five r-proteins (uL24, uL22, bL20, uL13, and uL4) essential for an early 50S-assembly stage, which cannot be bypassed for the formation of active 50S subunits, all bind near the 5′-end of the rRNA (Spillmann et al. 1977). Moreover, their in vitro order of incorporation neatly corresponds to their early incorporation determined in vivo (Chen and Williamson 2013).

Apart from one study on the mechanical action of bL20 (Mangeol et al. 2011), investigations about the mechanistic reasons why these early binders are essential are lacking. Moreover, it is still unknown why among the five early binders, uL24 stands out to initiate the cooperative assembly of the ribosomal large subunit (Nowotny and Nierhaus 1982).

To gain some understanding on these important topics, we have focused in this study on the interaction of the first large subunit r-protein binding to 23S rRNA in vivo—uL24 (Chen and Williamson 2013)—with its primary binding site

[4]**Present address:** Department of Chemistry, University of Michigan, Ann Arbor, Michigan 48109, USA

Corresponding authors: ulrich.bockelmann@inserm.fr, bizebard@ibpc.fr

Article is online at http://www.rnajournal.org/cgi/doi/10.1261/rna.067504.118.

© 2019 Geffroy et al. This article is distributed exclusively by the RNA Society for the first 12 months after the full-issue publication date (see http://rnajournal.cshlp.org/site/misc/terms.xhtml). After 12 months, it is available under a Creative Commons License (Attribution-NonCommercial 4.0 International), as described at http://creativecommons.org/licenses/by-nc/4.0/.

on the rRNA (Stelzl and Nierhaus 2001): a short 23S rRNA fragment whose structure is highly conserved in all kingdoms of life (Petrov et al. 2013), and which is essential for ribosome assembly in *E. coli* (Skinner et al. 1985; Stelzl and Nierhaus 2001). Very significantly, considering the assembly gradient hypothesis, this rRNA fragment is, among all specific r-protein binding sites, the site located nearest to the 5′ extremity of 23S rRNA (Spillmann et al. 1977). This rRNA fragment is at the same time the primary target of the essential r-protein uL4 (Stelzl et al. 2000), another early-binder whose presence is mandatory for the first step of *E. coli* 50S in vitro reconstitution (Spillmann et al. 1977). Structural and biochemical studies have shown that this small 23S rRNA fragment, which specifically interacts with only two r-proteins, uL4 and uL24, consists of helices H18, H19, H20 forming a three-way junction (Egebjerg et al. 1987; Stelzl and Nierhaus 2001; Noeske et al. 2015). All the aforementioned observations indicate that our in vitro studies focusing on this short RNA fragment encompassing the uL4/uL24 binding site provide a valuable approach to the initial stage of large ribosomal subunit assembly. It has been shown that single-molecule force measurements can shine new light on RNA–protein interactions (Mangeol et al. 2011; Koslover et al. 2012; Qu et al. 2012). Here we report on single-molecule force measurements performed on the rRNA fragment described above. We characterize the mechanical action of uL4 and uL24 and find that both proteins are able to individually stabilize the rRNA fragment. Moreover, we observe that this mechanical stabilization is enhanced when both proteins are bound simultaneously. Independently, we observe and quantify cooperative binding of uL4 and uL24. Taken together, these results illustrate a double property of uL4 and uL24 binding to their rRNA primary target: an rRNA structure stabilization enhancement and a cooperative binding for the same fragment. We propose that these two properties both contribute to the efficient stabilization of the rRNA local 3D structure.

RESULTS

A molecular construction containing the *E. coli* 23S rRNA fragment (from nucleotides 281 to 359) involved in the binding of the r-proteins uL4 and uL24 (Stelzl and Nierhaus 2001), flanked by two RNA/DNA handles (Fig. 1A), has been prepared as described in the Materials and Methods section. Linked to two μm-sized beads, the molecular construction is held in a dual optical trap (Fig. 1A). One trap is moved at constant velocity (50 nm/sec unless indicated otherwise) while the other is held fixed and used to measure the force.

Mechanical stabilization of the 23S rRNA fragment induced by uL4 and uL24

The stretching force versus displacement curves of our bare rRNA exhibits a sawtooth signal between 7 and 12 pN. Typically, 2 to 3 force drops of ~0.5 pN amplitude

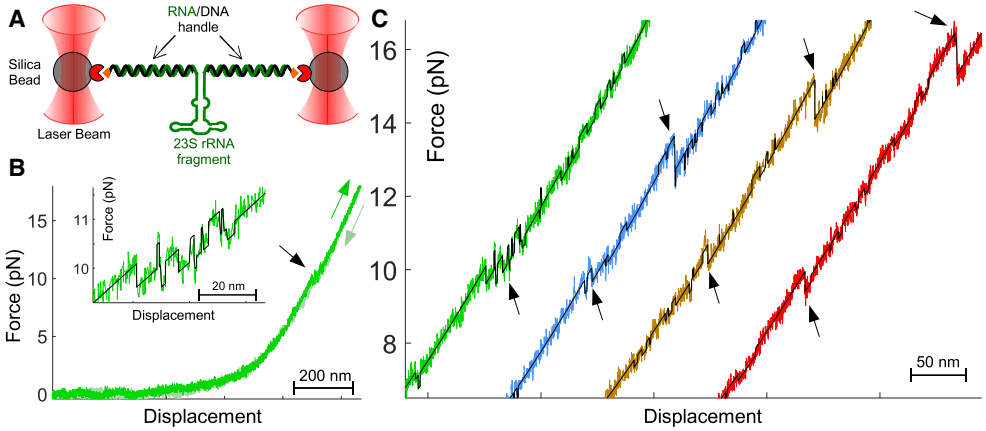

FIGURE 1. Typical force versus displacement curves. (*A*) A dual optical trap is used to manipulate a DNA/RNA molecular construction in a dumbbell configuration. In this configuration, the RNA containing the *E. coli* 23S rRNA fragment of interest (from nucleotides 281 to 359—secondary structure represented schematically) is hybridized to two DNA handles both containing a biotin moiety (orange) at one of their extremities. Biotin moieties are linked to streptavidin (red) coated silica beads. (*B*) Typical bare rRNA force versus displacement curve. As the molecular construction is stretched, one observes a sawtooth signal region around 10 pN (marked by the black arrow) corresponding to the progressive unfolding of the rRNA fragment of interest. Unfolding (green) and refolding (light green) curves as indicated by the corresponding arrows have been plotted showing little hysteresis. (*Inset*) A close-up shows the unfolding experimental sawtooth signal (green) and the idealized path (black) around 10 pN. (*C*) Region corresponding to the unfolding of the rRNA fragment of interest. A typical curve is represented for each set of experiments: bare rRNA fragment (green), rRNA fragment bound to uL4 (blue), rRNA fragment bound to uL24 (brown), rRNA fragment bound to both uL4 and uL24 (red). The curves have been shifted horizontally for better visualization. Arrows indicate most important force drops. In black are superimposed the idealized paths extracted from the analysis of the force versus displacement curves. These paths allow the precise assignation of the observed intermediate states during the progressive unfolding of the rRNA fragment of interest.

are observed—well above the experimental noise of ~0.2 pN—thus indicating the successive unfolding of rRNA structured intermediates (Fig. 1B,C, green curve). The curve before (after) the first (last) force drop corresponds to the elastic response of the molecular construction with the rRNA fragment of interest in the folded (fully unfolded) state. State to state transitions are frequently observed indicating that the unfolding occurs in a close-to-equilibrium condition (Mangeol et al. 2011).

When r-proteins are added at concentrations comparable or in excess over their dissociation constants (K_d) for the rRNA fragment ($K_d = 1/K_a$; see section "The r-proteins uL4 and uL24 bind cooperatively to the 23S rRNA fragment" describing K_a values and how they are determined from our experiments), a large fraction of the force versus displacement curves are different from the ones observed with bare rRNA—indicating protein binding. We have verified that this protein binding is specific to our investigated rRNA fragment via two negative control experiments described in the Supplemental Material.

Characteristically, when r-proteins are bound to the RNA, the sawtooth signal of the force vs. displacement curves extend to higher forces than when there is no protein bound (Fig. 1C). The first force drop observed still occurs around 10 pN indicating that the r-proteins do not play a role in the first rRNA intermediate stability. One still observes state to state transitions especially in the range of force between 7 and 12 pN. Interestingly, additional force drops are observed above 13 pN for uL4 and 14 pN for uL24 suggesting the existence of a mechanically stabilized rRNA partially unfolded state induced by the binding of the r-proteins. When uL4 together with uL24 are bound, a much more stabilized intermediate state above 15 pN is observed (Fig. 1C, red curve).

Hidden Markov modeling of the data identifies the intermediate states

Hidden Markov modeling (HMM) of the data has been implemented allowing for extracting reproducibly the intermediate states and the transition forces from the force versus extension curves.

The method relies on a fit of the data using the Worm-Like Chain (WLC) elasticity model (Marko and Siggia 1995; Odijk 1995). A first term is fitted to the data corresponding to the RNA/DNA handle elasticity curve. Then, a term modeling the elasticity of the single-stranded RNA is added. This allows converting the force versus displacement curve to the released single-stranded rRNA (ssRNA) length—i.e., corresponding to the progressive unfolding of the rRNA fragment of interest—as a function of displacement. All released ssRNA length versus displacement trajectories are then analyzed using the HMM software vbFRET (Bronson et al. 2009)—from which we have been able to extract the rRNA unfolding intermediate states and the values of the transition forces (as described in the Supplemental Material).

The released RNA length as a function of force is reported in a 2D histogram for the whole set of experiments without added r-proteins (Fig. 2A) and in the presence of both uL4 and uL24 at 8 μM each—i.e., in excess over their K_d values (Fig. 2B).

To confirm the validity of the vbFRET HMM analysis, the data have also been analyzed with the HMM software HaMMy (McKinney et al. 2006), and the corresponding 2D histograms have been plotted (Supplemental Fig. S1) for comparison with those obtained by the vbFRET software (Fig. 2). The two representations are similar, in particular regarding the intermediate states.

Intermediate states assignation

In the absence of r-proteins, the rRNA fragment exhibits two main partially unfolded states I_1 and I_2 (Fig. 2A). I_1 is located at 8 ± 2 nm which corresponds to the release of 14 ± 4 nucleotides of single-stranded RNA. I_1 is thus located in helix H18 of 23S rRNA (Fig. 2C). The existence and location of this intermediate can be rationalized using well-established RNA secondary structure prediction softwares and the WLC elasticity model (Supplemental Fig. S2). I_1 and F (the fully folded state) are populated together at forces below 10 pN. I_2 is located at 37 ± 2 nm, which corresponds to a release of 60 ± 4 nucleotides. I_2 is thus located beyond helix H18 and should correspond to the unfolding of either one of the two parallel helices, H19 or H20 (for clarity, I_2 is not represented in Fig. 2C, but is shown in Supplemental Fig. S3). I_2 is frequently observed especially in the range of force between 10 and 14 pN together with the fully unfolded state U.

In the presence of r-proteins, whether uL4 or uL24 (Supplemental Fig. S4a,b) or both (Fig. 2B), I_1 is still observed, while the contribution of I_2 is strongly reduced concomitant with the occurrence of I_3. I_3 is observed only rarely in the absence of r-proteins. It is located at 17 ± 5 nm which corresponds to the release of 28 ± 8 nucleotides. I_3 can thus be assigned very close to the junction between the three helices H18, H19 and H20 (Fig. 2C). Its location is in agreement with the identification of the minimal RNA fragment that contains the binding sites of both uL4 and uL24 (Stelzl et al. 2000) as shown in Figure 2D.

From this analysis, we conclude that the two r-proteins uL4 and uL24, individually as well as both together, stabilize an intermediate state localized very close to the junction between the three helices H18, H19, and H20.

The binding of both proteins uL4 and uL24 provides an enhanced mechanical stabilization of the 23S rRNA fragment

Here, we focus on the mechanical stabilization of the protein-stabilized intermediate state I_3. To quantify this effect,

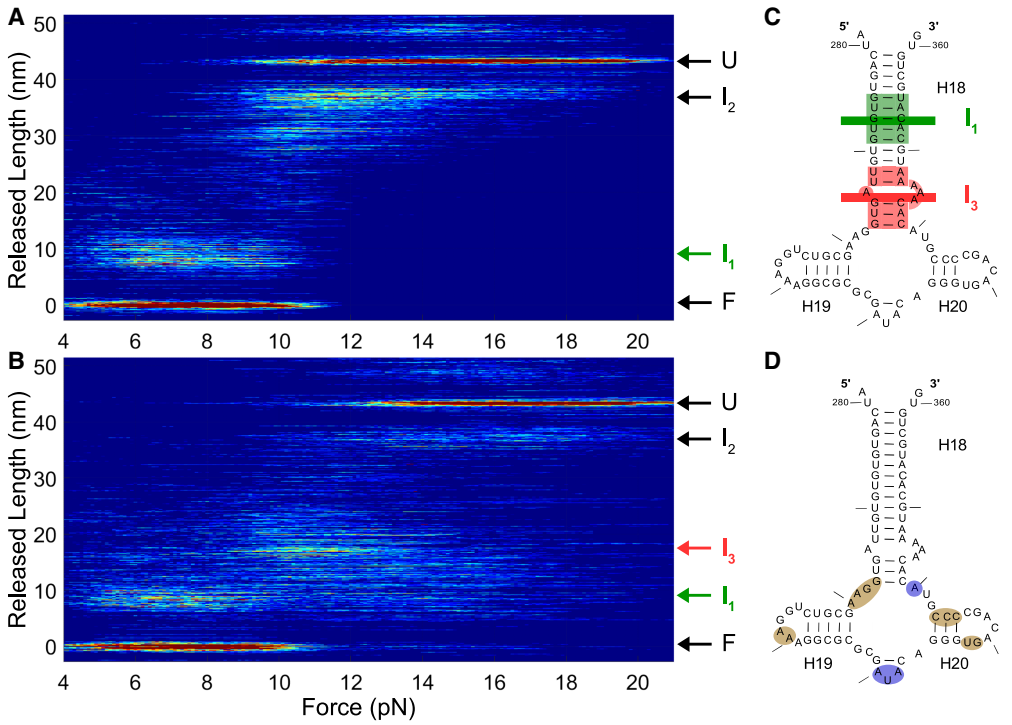

FIGURE 2. (*A*) Superposition of the idealized paths of all the measurements performed without r-proteins (254 measurements). All the curves have been superimposed in a heat map histogram where red (dark blue) indicates frequently (rarely) observed states. (*B*) Superposition of the idealized paths of all the measurements performed with 8 µM of each r-protein uL4 and uL24 (255 measurements). (*C*) Secondary structure of the rRNA fragment. The colored bars (areas) indicate the mean position (standard deviation) of the two RNA unfolding intermediate states I_1 and I_3 located in H18. (*D*) Secondary structure of the rRNA fragment of interest showing nucleotides involved in RNA/uL24 (brown) and RNA/uL4 (blue) contacts observed in the fully assembled 50S ribosomal subunit (analyzed from PDB entry 4YBB).

we have determined a typical force of stabilization of the intermediate in the different experimental conditions (i.e., in the presence/absence of either r-protein). The whole experimental procedure to determine these values is detailed in the Supplemental Material.

Fitted values of stabilization forces of the intermediate I_3 are reported in Figure 3—alongside the experimental histograms from which these values have been extracted.

From these figures, it is clearly apparent that the presence of either one of the two r-proteins provides a mechanical stabilization of the intermediate state. The mean force needed to unfold the rRNA fragment rises from 10.3 pN without r-protein to 13.0 pN in the presence of uL4 and 14.6 pN in the presence of uL24 (see Fig. 3A–C). The presence of both r-proteins together provides a stabilization to 15.8 pN (Fig. 3D). This result indicates that uL4 and uL24 act additively to provide an extra-stabilization of the rRNA fragment.

The r-proteins uL4 and uL24 bind cooperatively to the 23S rRNA fragment

The methodology used in the previous paragraph can also be used to extract the binding affinities of the two proteins for the rRNA fragment (see Supplemental Fig. S5 and Supplemental Material section "Estimation of the r-proteins' affinities…" for the detailed procedure). First, binding affinities were determined from experiments where we varied the concentration of one protein in the absence of the other. In our experimental conditions, the corresponding association constants are the following: $K_a^{uL24} = 0.06\ \mu M^{-1}$ and $K_a^{uL4} = 1.5\ \mu M^{-1}$ (see Fig. 4).

Second, from measurements in the presence of both uL4 and uL24 at different concentrations, we can also quantify affinities of one protein in the presence of the other: The corresponding values are also shown in Figure 4.

From these affinity measurements, it appears that uL4 and uL24 bind cooperatively to the 23S rRNA fragment (we observe a sevenfold enhancement of the affinity of uL4 when uL24 is already bound; and a 5.5-fold enhancement of the affinity of uL24 when uL4 is already bound). The similarity of these last two figures suggests that the binding of the two proteins can be modeled using the minimal cooperative binding scheme displayed in Figure 4.

Assembly initiator role of uL24

As already mentioned, a major biological difference between uL4 and uL24 is that uL24 acts as an assembly initiator and uL4 does not (Nowotny and Nierhaus 1982). Is it

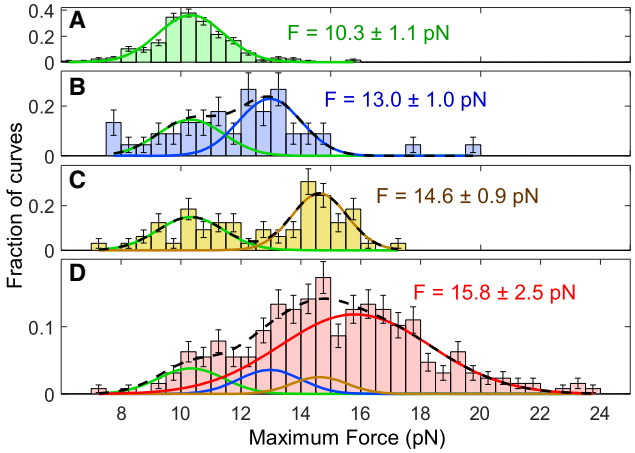

FIGURE 3. Histograms of the maximum force reached by states of released length below 25 nm (region corresponding to F, I_1, and I_3) for experiments performed (*A*) without r-protein (254 measurements), (*B*) with uL4 at 8 µM (45 measurements), (*C*) with uL24 at 15 µM (65 measurements), (*D*) with both uL4 and uL24 at 8 µM each (255 measurements). Each bar represents the fraction of curves where the maximum force reached by the intermediates occurs in the corresponding force range (with standard errors pictured as error bars). To determine the typical force necessary to unfold each possible rRNA fragment-protein complex, each distribution of forces displayed in panels *A*–*D* has been fitted as the sum of gaussians (the procedure is thoroughly described in our Supplemental Material paragraph "Estimation of the typical force involved in the mechanical stabilization"). In panel *A*, where there is no protein, the distribution of forces has been fitted using a single Gaussian (green curve) and the characteristic force is displayed in green. This gaussian is used subsequently for panels *B*–*D*. In panels *B* and *C*, where only one of the two proteins is present in solution, each distribution is the sum of two gaussians (one displayed in green: no protein bound [previously determined]; and one in blue or brown [uL4- or uL24-bound RNA fragment, respectively]). In panel *D* (the two proteins in solution), the distribution is fitted by a model which is the sum of four gaussians, corresponding to the four possible cases: no protein, uL4 bound, uL24 bound, uL4 + uL24 bound. The first three of them were previously determined. The fourth gaussian is newly determined and shown in red. In panels *B*–*D*, the sum of the gaussians is represented as a dashed line and thus corresponds to the best fit to the complete data. The mean force of each gaussian is indicated.

possible to understand this difference within our experimental configuration? To address this question we performed two different sets of experiments. In the first set (see "Order of incubation" section in the Supplemental Material for details), we performed successive incubations of the rRNA fragment first with uL4, then uL24—or vice versa: The experimental outcome was not significantly different in the two cases (Supplemental Fig. S6a,b). The conclusion is that if a difference exists it does not persist beyond the time resolution that we could achieve in this set of experiments, which was 15–30 min. In the second set of experiments, we performed incubation with uL4 and uL24 together, but varied their concentrations. Here we looked specifically for an asymmetry in the binding properties of the two proteins (for instance that a small concentration of uL24 would significantly enhance the binding affinity of uL4, while a small concentration of uL4 would less enhance the binding affinity of uL24). In view of the uncertainties of the K_a values presented in Figure 4 and Supplemental Figure S5, we note that such difference might well be not statistically significant. Restricting ourselves to the mean K_a values presented in the same figures, we find that the association constant K_a for uL4 increased by a factor seven when uL24 is already bound, while K_a for uL24 increased by a smaller factor of about five when uL4 is already bound.

DISCUSSION

uL4 and uL24 both stabilize the rRNA fragment

Our force measurements allowed us to characterize the different mechanical properties of the bare RNA fragment and the 3 RNA/protein complexes.

The bare rRNA fragment displays partially unfolded states (Fig. 2) whose locations are compatible with the RNA 3D structure observed in the fully assembled 50S subunit (Fig. 5). The forces needed to completely unwind this RNA are in the range 7–12 pN—as expected from values found in the literature (Harlepp et al. 2003; Tinoco et al. 2006; Mangeol et al. 2011). When uL4 or uL24 are present in the solution, the first observed states F and I_1 still unwind in the 7–12 pN range (in agreement with the observation that none of the proteins binds to the corresponding RNA region), but to break the next encountered intermediate I_3 requires higher forces (≥13 pN) than with the bare RNA. Our analysis maps the location of this unwinding intermediate very close to the three-way junction contacted by both proteins (Figs. 2D, 5).

Inspection of the 50S 3D structure helps to rationalize this observation (Fig. 5; Supplemental Fig. S7). As each protein directly contacts two strands involved in the H18/H19/H20 three-way junction, separation of these strands

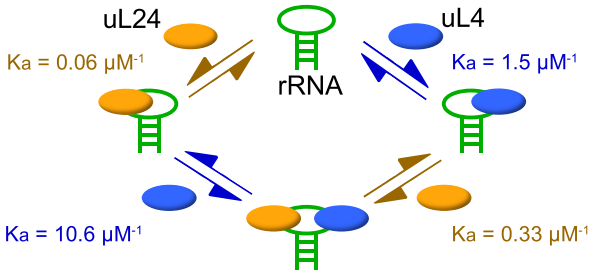

FIGURE 4. Minimal cooperative binding scheme of r-proteins uL4 and uL24 to the rRNA fragment: Association constants directly measured from our data are indicated (i.e., 0.06 ± 0.01 μM^{-1} for uL24; 1.5 ± 0.2 μM^{-1} for uL4; 0.33 ± 0.01 μM^{-1} for uL24 when uL4 is already bound to the rRNA fragment; 10.6 ± 3.5 μM^{-1} for uL4 when uL24 is already bound to the rRNA fragment; all figures correspond to mean ± standard error).

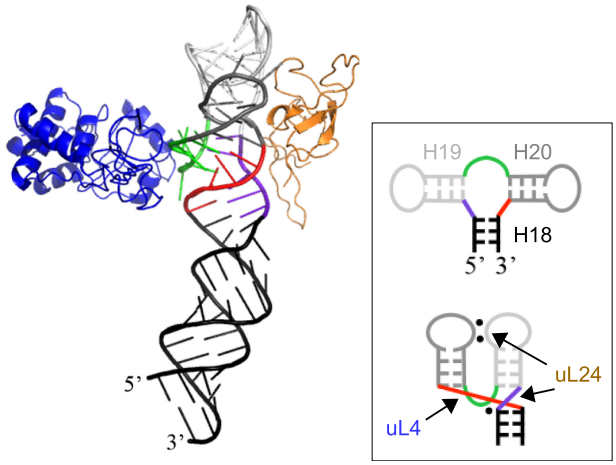

FIGURE 5. Ribbon representation of the 3D structure of the RNA and proteins investigated in this paper—structure as it is observed in the fully assembled 50S subunit (PDB entry 4YBB). The RNA is colored following the conventions shown in the *inset*; the r-proteins uL4 and uL24 are pictured in blue and orange respectively. (*Inset*) Color conventions used to highlight the H18/H19/H20 three-way junction: *top*, 2D representation of the junction; *bottom*, schematic representation of the 3D structure of the junction—a prototypic Y-shaped three-way junction, as described in the text. In this picture are also shown schematically the tertiary interactions that stabilize this particular 3D structure: RNA–RNA interactions (black dots) and protein–RNA interactions (arrows).

needs higher force when a protein is bound with respect to bare rRNA. Interestingly, when only uL4 is bound, the stabilized intermediate state is the same as when only uL24 is bound—despite the fact that uL24 binds the two strands under mechanical tension, and uL4 only binds one of them. Our observation that the intermediate stabilized is the same in both cases indicates that the mechanical stability of the folded three-way junction indeed depends on the three strands (violet, green and red in Fig. 5). This is probably due to the many close contacts between them: They are not independent and mechanically unfold as a unique structure. Noteworthy, forces needed are systematically higher when uL24 is the one protein present in solution—consistent with the observation that uL24 makes overall more close contacts with the rRNA fragment than does uL4. When both proteins are bound simultaneously, the force needed to unwind I_3 is even higher than previously (≥15 pN). The mechanical stability enhancement of this three-way junction due to the binding of uL4 and uL24 indicates that under mechanical tension, the two proteins pop off together and not independently.

Mode of action of uL4 and uL24

First, the observed intermediates of RNA unfolding by force are mostly the same in the presence and absence of either protein and these intermediates can be mapped on the RNA 3D structure of the mature ribosome (Fig. 2). Second, we observe that the force curves recorded during refolding of the RNA fragment (induced by decreasing trap separation) are not changed by the presence of uL4 and uL24 (Supplemental Fig. S8), suggesting that the proteins do not assist refolding (they are clamps rather than chaperones).

Information from the literature or from RNA structure prediction software also suggests that the 3D conformation of the RNA fragment as observed in the assembled 50S is similar to the one adopted by the RNA on its own: First, the secondary structure of this RNA is almost exactly predicted by diverse prediction programs (e.g., Mfold [Zuker 2003], Vienna RNAfold [Gruber et al. 2008]); second, the 3D structure of the free RNA is compatible with chemical/enzymatic probing (Egebjerg et al. 1987; Stelzl and Nierhaus 2001); third, this RNA fragment adopts (in the ribosome) a very commonly encountered RNA 3D structure—an archetypal Y-shaped three-way junction (Fig. 5 inset), which is well established to be stably folded on its own (without any protein) (de la Peña et al. 2009). Overall, these arguments favor the interpretation that the RNA fragment nearly adopts its final 3D structure without the proteins, but that uL4 and uL24 act together to strongly stabilize this particular RNA 3D conformation (Fig. 5).

Our observations are thus compatible with a structural model where uL4 and uL24 act as molecular clamps rather than RNA chaperones, stabilizing an already folded RNA 3D structure.

Cooperative binding of uL4 and uL24 to their rRNA target

The cooperativity of the ribosomal assembly process in vitro (and very probably also in vivo) has been discussed in the literature (Nowotny and Nierhaus 1982) and its biological importance emphasized. This cooperativity should help to achieve the high efficiency of the ribosomal assembly process in vivo and is probably mandatory in the common cellular context where rRNAs are in molar excess over r-proteins (Nowotny and Nierhaus 1982).

The cooperativity has been quantified for small subunit r-proteins binding to 16S rRNA (Recht and Williamson 2004). However, binding cooperativity has never been quantified for large subunit r-proteins. In this paper, we show the cooperative binding of uL4 and uL24 to their primary target on 23S rRNA and quantify it. The resulting figure (approximately sixfold enhancement of the binding of one protein when the other is already bound—see Fig. 4) is very significant—i.e., much higher than 1. The molecular mechanism of this cooperative binding can be assessed by inspection of the 3D structure of the complex uL4/uL24/RNA as observed in the fully assembled 50S subunit (Supplemental Fig. S7): The two proteins do not interact directly but several indirect interactions are mediated through target RNA base pairs. In this case, it is likely

that binding of one protein to these nucleotides will alter their local dynamics, which in turn will favor the binding of the other protein.

Efficient stabilization of the rRNA fragment

The mechanical stabilizations expressed in pN (Fig. 3) and the binding affinities expressed in μM^{-1} (Fig. 4) are different quantities and describe different properties. A protein could provide weak mechanical stabilization and have high affinity. It could provide strong mechanical stabilization and have low affinity (Bustamante et al. 2004; Seidel and Dekker 2007).

Regarding the combined action of two proteins, enhanced mechanical stabilization (Fig. 3) and cooperative binding (Fig. 4) are different properties as well. In the specific case of uL4 and uL24 investigated in this work, these two properties lead to an efficient stabilization of the RNA fragment. First, each protein directly affords a mechanical stabilization of the folded RNA molecule and the binding of both even more stabilizes this RNA. Second, the cooperative binding of the two proteins ensures that this extra- stabilized species will occur more frequently.

Mechanical stabilization of the uL4/uL24-bound rRNA fragment: possible biological implications

The small RNA region investigated in this paper is essential for ribosome assembly (Skinner et al. 1985); and the two proteins uL4 and uL24 are essential for the formation of the first in vitro assembly intermediate (Nowotny and Nierhaus 1982).

A biological interpretation of our experimental results is that the stabilization afforded by r-proteins of rRNA local 3D structure against destabilization by force would be necessary during coupled rRNA transcription and ribosomal subunit assembly. Our experimental pulling on the ends of an RNA molecule could mimic the forces occurring during ribosome assembly in vivo. Profound conformational changes occur during assembly, which implies that local tension develops transiently.

Our force measurement data suggest that uL4 and uL24 binding energetically stabilizes the folded 3D structure of the investigated rRNA fragment. This stabilization by uL4 and uL24 is similar to what has been shown for another essential early-binding r-protein acting as a clamp (bL20) (Mangeol et al. 2011) (interestingly, bL20 and uL24 are both strict assembly proteins, which can be harmlessly removed from the 50S subunit once assembled and thus have no other role in the mature particle [Nierhaus 1991; Stelzl and Nierhaus 2001]). A possible interpretation of the stabilization afforded by these early binder clamps is that this would help stabilizing and/or funneling 23S rRNA (and 50S) into the native functional structure. In vivo, this proposed role of early-binding r-proteins would be especially relevant to the assembly gradient hypothesis: As soon as the rRNA is transcribed, its correct 3D conformation is stabilized by r-proteins—effectively reducing the number of degrees of freedom available to the rRNA molecule during the folding process.

Why is uL24 an assembly initiator and uL4 is not?

We observe a small asymmetry in the enhancement of the binding affinity of one protein provided by prior binding of the other protein (see paragraph "Assembly initiator role of uL24" in the Results section). This observation could be an element favoring uL24 as initiator, although we must note that the experimentally observed asymmetry is relatively small in magnitude and within experimental uncertainty.

In view of uL24's role as assembly initiator, it is surprising that this protein exhibits a significantly weaker affinity to its primary 23S target sequence than does uL4 (ratio of 25 between the K_a values, see Fig. 4). On the other hand, we observe a quantitative difference in the force stabilization of the rRNA fragment afforded by one protein compared to the other (14.6 pN for uL24 vs 13.0 pN for uL4).

Based on these findings, we propose two possibilities. First, that the observed superior force stabilization afforded by uL24 is directly associated with the biological role of the assembly initiator. Second, that the asymmetry between the roles of the two proteins might originate not from equilibrium properties but from kinetic properties—for example, uL24 would dissociate more slowly once bound to its RNA target than uL4. We note that the two possible models are not mutually exclusive. Indeed, ribosome assembly involves profound conformational changes in RNA structure, which implies that high mechanical tension arises transiently. An assembly initiator protein must dissociate slowly enough to allow subsequently binding assembly proteins to fix and it must be able to fulfill this role in the presence of force.

We believe that our single-molecule force measurements provide new elements on the question of this subsection, but they do not provide a simple answer. It is well possible that part of the full picture lies beyond the investigated system of uL24, uL4 and the 281–359 fragment of the 23S RNA.

Inspection of the 3D structure of the 50S and examination of the interactions of the 281–359 fragment, uL4 and uL24 with the rest of the subunit reveals a number of interesting points. The assembly initiator protein uL24 contacts three short segments of 23S rRNA (all located close to the 5′ extremity of this RNA), but, as stated previously, the 281–359 fragment is its primary target in vitro and in vivo. Possibly, uL24 first binds to this fragment, then to the other two 23S segments—and, as such, the assembly initiator plays its role by stabilizing strongly the

local 3D structure, including the RNA–RNA contacts between the three segments. In view of the literature (Spillmann et al. 1977; Chen and Williamson 2013), one can postulate that, a little later during the assembly process, uL4 binds to the 281–359 fragment, further stabilizing its 3D structure. This interaction should also anchor correctly uL4, which, contrary to uL24, interacts with many other parts of the assembled 50S structure and has not only an assembly role, but also a functional role in the ribosome (Nikolay et al. 2015).

MATERIALS AND METHODS

RNA molecular constructions

The single-stranded RNA sequence of interest (nucleotides 281 to 359 of *E. coli* 23S rRNA), flanked by two RNA/DNA handles of 2.5 and 3 kilo-base pairs labeled with biotin moieties, is attached to two 0.96 µm diameter silica beads coated with streptavidin (Polysciences, Inc.) as described previously (Geffroy et al. 2018)—with the exception of the primers used for the PCR reaction, which were the following:

Primer-forward: 5′ - tca ggc tct ggg ctg ctc ccc

Primer-backward: 5′ - agc tcg atg agt agg gcg gga

Overexpression and purification of *E. coli* r-proteins uL4 and uL24

The rplD or rplX gene encoding uL4 or uL24 from *E. coli* strain A19 was cloned into the pET-15b-SUMO expression vector, possessing His_6 tag and SUMO (small ubiquitin-like modifier) downstream from the T7 promoter site of pET-15b. The Rosetta(DE3)pLysS derivative carrying the above plasmids was grown in LB containing 100 µg/mL ampicillin and 25 µg/mL chloramphenicol.

Proteins uL4 or uL24 were overexpressed in the *E. coli* strain Rosetta(DE3)pLysS (Novagen) after 3 h IPTG induction at 37°C. Cells overexpressing uL4 or uL24 were sonicated in lysis buffer (400 mM KCl, 20 mM $MgCl_2$, 50 mM Tris-HCl pH 7.6, 4 M Urea and 7 mM β-mercaptoethanol for uL4, 1 M NH_4Cl, 10 mM $MgCl_2$, 50 mM Tris-HCl pH 7.6, 7 mM β-mercaptoethanol for uL24) and the extract was centrifuged at 20,000*g* for 45 min. After centrifugation, the protein was purified by nickel column. After removing the His_6 tag-SUMO by Ulp1 digestion and reverse his tag purification by nickel column, the protein was dialyzed against ion exchange buffer (100 mM KCl, 10 mM $MgCl_2$, 50 mM Tris-HCl pH 7.6, 4 M Urea and 7 mM β-mercaptoethanol for uL4, 200 mM KCl, 10 mM $MgCl_2$, 50 mM Tris-HCl pH 7.6, 7 mM β-mercaptoethanol for uL24) and further purified on Mono S column using a 100–400 mM KCl gradient for uL4, 200–600 mM KCl gradient for uL24. The purity of all proteins was analyzed by SDS-PAGE and confirmed that there are no extra bands (Supplemental Fig. S9). Collected protein was dialyzed against storage buffer (1 M KCl, 10 mM $MgCl_2$, 50 mM Tris-HCl pH 7.6, 30% glycerol and 7 mM β-mercaptoethanol for uL4; 1 M KCl, 20 mM $MgCl_2$, 50 mM Tris-HCl pH 7.6, 30% glycerol and 7 mM β-mercaptoethanol for uL24). Aliquots of the proteins were frozen at −80°C.

Single-molecule force measurements: setup, measurements and data analysis

The dual optical trap consists of two beams emerging from the same laser source (1064 nm, 2W) as in (Mangeol and Bockelmann 2008). Force measurements have been performed at 29°C in 400 mM KCl, 20 mM Hepes Na pH 7.6, 5 mM $MgCl_2$, and 0.1% (w/v) biotinylated PEG 5000 (Laysan Bio, Inc.) at sampling rate of 300 Hz with an anti-aliasing filter at 132 Hz. The buffer conditions are highly similar to the ones used by Nierhaus and Dohme in their in vitro 50S subunit reconstitution assays (Nierhaus and Dohme 1974) with the additional inclusion of PEG which proved mandatory to avoid adsorption of r-proteins to the beads and was indeed a key point in the success of our experiments.

Force versus displacement data were analyzed with custom scripts written in Matlab (MathWorks). Additionally, HMM of these data was implemented, allowing for extracting reproducibly the rRNA unfolding intermediate states and the values of the transition forces. The HMM step was carried out using either one of two publicly available HMM programs: vbFRET (Bronson et al. 2009) or HaMMy (McKinney et al. 2006). The complete methodology is detailed in the Supplemental Material.

SUPPLEMENTAL MATERIAL

Supplemental material is available for this article.

ACKNOWLEDGMENTS

We thank Dr. M. Dreyfus for fruitful discussions. This work has benefited immensely from the contribution of our friend and colleague Knud Nierhaus. It is dedicated to his memory. This work was supported by the Human Frontier Science Program (RGP008/2014).

Received May 29, 2018; accepted January 19, 2019.

REFERENCES

Bronson JE, Fei J, Hofman JM, Gonzalez RL, Wiggins CH. 2009. Learning rates states from biophysical time series: a Bayesian approach to model selection single-molecule FRET data. *Biophys J* **97:** 3196–3205. doi:10.1016/j.bpj.2009.09.031

Bustamante C, Chemla YR, Forde NR, Izhaky D. 2004. Mechanical processes in biochemistry. *Annu Rev Biochem* **73:** 705–748. doi:10.1146/annurev.biochem.72.121801.161542

Chen SS, Williamson JR. 2013. Characterization of the ribosome biogenesis landscape in *E. coli* using quantitative mass spectrometry. *J Mol Biol* **425:** 767–779. doi:10.1016/j.jmb.2012.11.040

de la Peña M, Dufour D, Gallego J. 2009. Three-way RNA junctions with remote tertiary contacts: a recurrent highly versatile fold. *RNA* **15:** 1949–1964. doi:10.1261/rna.1889509

Egebjerg J, Leffers H, Christensen A, Andersen H, Garrett RA. 1987. Structure accessibility of domain I of *Escherichia coli* 23 S RNA in free RNA, in the L24-RNA complex in 50 S subunits. Implications for ribosomal assembly. *J Mol Biol* **196:** 125–136. doi:10.1016/0022-2836(87)90515-8

Geffroy L, Mangeol P, Bizebard T, Bockelmann U. 2018. RNA unzipping force measurements with a dual optical trap. *Methods Mol Biol* **1665:** 25–40. doi:10.1007/978-1-4939-7271-5_2

Gruber AR, Lorenz R, Bernhart SH, Neuboeck R, Hofacker IL. 2008. The Vienna RNA Websuite. *Nucleic Acids Res* **36:** W70–W74. doi:10.1093/nar/gkn188

Harlepp S, Marchal T, Robert J, Léger JF, Xayaphoummine A, Isambert H, Chatenay D. 2003. Probing complex RNA structures by mechanical force. *Eur Phys J E Soft Matter* **12:** 605–615. doi:10.1140/epje/e2004-00033-4

Herold M, Nierhaus KH. 1987. Incorporation of six additional proteins to complete the assembly map of the 50S subunit from *Escherichia coli* ribosomes. *J Biol Chem* **262:** 8826–8833.

Koslover DJ, Fazal FM, Mooney RA, Landick R, Block SM. 2012. Binding translocation of termination factor Rho studied at the single-molecule level. *J Mol Biol* **423:** 664–676. doi:10.1016/j.jmb.2012.07.027

Mangeol P, Bockelmann U. 2008. Interference crosstalk in double optical tweezers using a single laser source. *Rev Sci Instrum* **79:** 083103. doi:10.1063/1.2957652

Mangeol P, Bizebard T, Chiaruttini C, Dreyfus M, Springer M, Bockelmann U. 2011. Probing ribosomal protein-RNA interactions with an external force. *Proc Natl Acad Sci* **108:** 18272–18276. doi:10.1073/pnas.1107121108

Marko JF, Siggia ED. 1995. Stretching DNA. *Macromolecules* **28:** 8759–8770. doi:10.1021/ma00130a008

McKinney SA, Joo C, Ha T. 2006. Analysis of single-molecule FRET trajectories using hidden Markov modeling. *Biophys J* **91:** 1941–1951. doi:10.1529/biophysj.106.082487

Nierhaus KH. 1991. The assembly of prokaryotic ribosomes. *Biochimie* **73:** 739–755. doi:10.1016/0300-9084(91)90054-5

Nierhaus KH, Dohme F. 1974. Total reconstitution of functionally active 50S ribosomal subunits from *Escherichia coli*. *Proc Natl Acad Sci* **71:** 4713–4717. doi:10.1073/pnas.71.12.4713

Nikolay R, van den Bruck D, Achenbach J, Nierhaus KH. 2015. Ribosomal proteins: role in ribosomal functions. In *eLS*. Wiley, Chichester. doi:10.1002/9780470015902.a0000687.pub4

Noeske J, Wasserman MR, Terry DS, Altman RB, Blanchard SC, Cate JHD. 2015. High-resolution structure of the *Escherichia coli* ribosome. *Nat Struct Mol Biol* **22:** 336–341. doi:10.1038/nsmb.2994

Nowotny V, Nierhaus KH. 1982. Initiator proteins for the assembly of the 50S subunit from *Escherichia coli* ribosomes. *Proc Natl Acad Sci* **79:** 7238–7242. doi:10.1073/pnas.79.23.7238

Odijk T. 1995. Stiff chains filaments under tension. *Macromolecules* **28:** 7016–7018. doi:10.1021/ma00124a044

Petrov AS, Bernier CR, Hershkovits E, Xue Y, Waterbury CC, Hsiao C, Stepanov VG, Gaucher EA, Grover MA, Harvey SC, et al. 2013. Secondary structure domain architecture of the 23S 5S rRNAs. *Nucleic Acids Res* **41:** 7522–7535. doi:10.1093/nar/gkt513

Qu X, Lancaster L, Noller HF, Bustamante C, Tinoco I. 2012. Ribosomal protein S1 unwinds double-stranded RNA in multiple steps. *Proc Natl Acad Sci* **109:** 14458–14463. doi:10.1073/pnas.1208950109

Recht MI, Williamson JR. 2004. RNA tertiary structure cooperative assembly of a large ribonucleoprotein complex. *J Mol Biol* **344:** 395–407. doi:10.1016/j.jmb.2004.09.009

Seidel R, Dekker C. 2007. Single-molecule studies of nucleic acid motors. *Curr Opin Struct Biol* **17:** 80–86. doi:10.1016/j.sbi.2006.12.003

Skinner RH, Stark MJ, Dahlberg AE. 1985. Mutations within the 23S rRNA coding sequence of *E. coli* which block ribosome assembly. *EMBO J* **4:** 1605–1608. doi:10.1002/j.1460-2075.1985.tb03824.x

Spillmann S, Dohme F, Nierhaus KH. 1977. Assembly *in vitro* of the 50 S subunit from *Escherichia coli* ribosomes: proteins essential for the first heat-dependent conformational change. *J Mol Biol* **115:** 513–523. doi:10.1016/0022-2836(77)90168-1

Stelzl U, Nierhaus KH. 2001. A short fragment of 23S rRNA containing the binding sites for two ribosomal proteins, L24 and L4, is a key element for rRNA folding during early assembly. *RNA* **7:** 598–609. doi:10.1017/S1355838201002059

Stelzl U, Spahn CMT, Nierhaus KH. 2000. Selecting rRNA binding sites for the ribosomal proteins L4 and L6 from randomly fragmented rRNA: application of a method called SERF. *Proc Natl Acad Sci* **97:** 4597–4602. doi:10.1073/pnas.090009297

Tinoco I, Li PTX, Bustamante C. 2006. Determination of thermodynamics kinetics of RNA reactions by force. *Quart Rev Biophys* **39:** 325–360. doi:10.1017/S0033583506004446

Zuker M. 2003. Mfold web server for nucleic acid folding hybridization prediction. *Nucleic Acids Res* **31:** 3406–3415. doi:10.1093/nar/gkg595